

# Aerodynamic Performances of MAV Wing Shapes

N. I. Ismail\*, A. H. Zulkifli, H. Yusoff, R. J. Talib, A.R.  
Hemdi, N. M. Muzammil N. Mustapa

Faculty of Mechanical Engineering, Universiti Teknologi  
MARA (Pulau Pinang), 13500 Pulau Pinang, Malaysia.

\*iswadi558@ppinang.uitm.edu.my

## ABSTRACT

*In general, there are four common Low Reynolds Number wing's designs for fixed wing Micro Air Vehicle (MAV) which known as Rectangular, Zimmerman, Inverse Zimmerman and Ellipse wing. However, each wing design produces diverse performance and in fact the aerodynamic comparison study among the wings is still lack. Thus, the objective of this study is to evaluate the basic aerodynamic performance found on Rectangular, Zimmerman, Inverse Zimmerman and Ellipse wing designs with view to find the optimal wing shape for Micro Air Vehicle (MAV) configuration. Here, each design was analysed based on simulation works. The results show that at stall angle, the Ellipse wing has maximum lift coefficient ( $C_{L_{max}}$ ) recorded at 1.12 which is at least 4.33% higher than the other wing designs. Based on drag coefficient ( $C_D$ ) analysis, the Inverse Zimmerman Wing exhibited the lowest minimum drag value at 0.033 which is 8.45% lower than the other wing's designs. In moment coefficient analysis, the results reveal that the Inverse Zimmerman Wing has produced the steepest curve slope value at -0.36 which is 17.39% higher than the other wings. The aerodynamic efficiency ( $C_L/C_D$ ) study has also revealed that Zimmerman Wing recorded the highest  $C_L/C_D$  value at 6.80 and at least 1.35% higher than to the other wing. Based on these results, it was concluded that Zimmerman wing has the highest potential to be adopted as MAV wing due to its optimal aerodynamic efficiency.*

**Keywords:** *Micro Air Vehicle, Zimmerman, Inverse Zimmerman and Ellipse wing.*

## **Introduction**

Micro Air Vehicle or MAV is a class of relatively small and light-weight Unmanned Aerial Vehicle. MAV was created to be practically operated in situations that are unsuitable for large aircraft such as reconnaissance mission, situational awareness and air sampling [1]. In recent years, there has been an interest in MAV with a largest linear dimension no greater than 30 centimetres [2]. Modern MAV usually weight in between 50 to 250 gram and its operating cruise speed is typically between 5 m/s to 23 m/s [3]. MAV can be categorized into different types based on its wing design and performances for example: fixed-wing MAV, rotary wing MAV, and flapping wing MAV [4]. Fixed-wing MAV is the most popular choices among researcher because of its straightforward design and it offers better payload [5]. Fixed-wing MAVs operate in between  $10^4 \sim 10^5$  Reynolds Number, thus it exhibits a unique aerodynamic performance during flight such as high stall-angles of attack, low lift-to-drag ratio, large wing tip vortex swirling, difficult flight controllability and small centre of gravity range [6]. Moreover, fixed-wing MAVs flight characteristics such as lift-to-drag ratio and angle of attack (AoA) change considerably from its larger counterpart (UAV) upon entering the Low Reynolds Number regime. As result, fixed-wing MAVs are hard to control and difficult to achieve a desirable flight range, endurance and cruise speed [7]. Therefore, several types of wing shape design for fixed-wing MAV has been introduced with view to improve the lift and lift-to-drag ratio characteristics [8]. The most common wing shapes adopted for fixed-wing MAV wing are known as Rectangular, Zimmerman, Inverse Zimmerman, and Elliptical [9]. However, the previous researches [9]–[12] had shown that the aerodynamic evaluation on such aforementioned wings have been done separately. As a result, the aerodynamics comparison study among the selected MAV wing shapes is still lacks. Thus, the overall aim of current study is to compare the aerodynamic performances (lift, drag and moment coefficient) between the Rectangular, Zimmerman, Inverse Zimmerman, and Elliptical wings. In this works, the aerodynamic performances of each MAV wing are analysed based on virtual wind tunnel simulation by using ANSYS-CFX software. The results for each wing will be compared to elucidate the benevolent performances of each wing and its suitability to be adopted as fixed-wing MAV platform.

## **Methodology**

### **MAV wing model**

In this works, only as Rectangular, Zimmerman, Inverse Zimmerman and Elliptical shape designs is used for current analysis. The basic dimensions and shapes of each wing are given in Fig.1 to 4. The wing shape selection is

based on its commonly used as fixed-wing MAV platform. Basically, all wing has similar aspect ratio ( $AR=1.5$ ), thickness (1.0mm), maximum camber value (6% of chord), location of maximum camber ( $x/c = 0.3$ ) and wingspan (150mm). The difference between them is the only the platform shape.

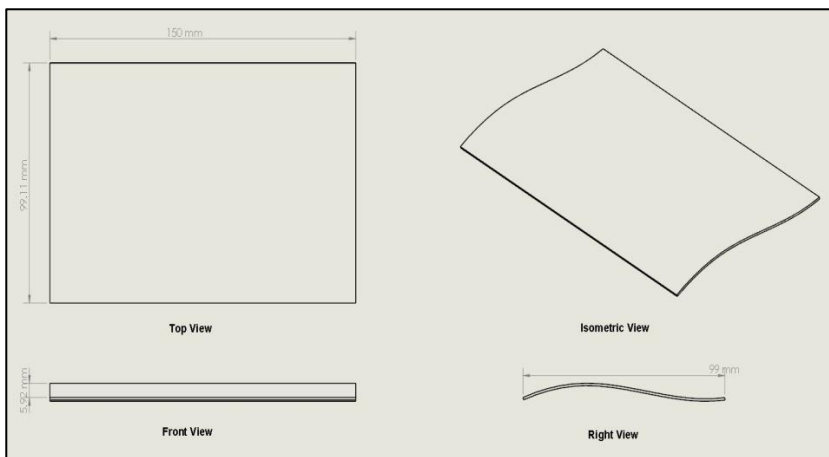


**Fig 1. Rectangular Wing**

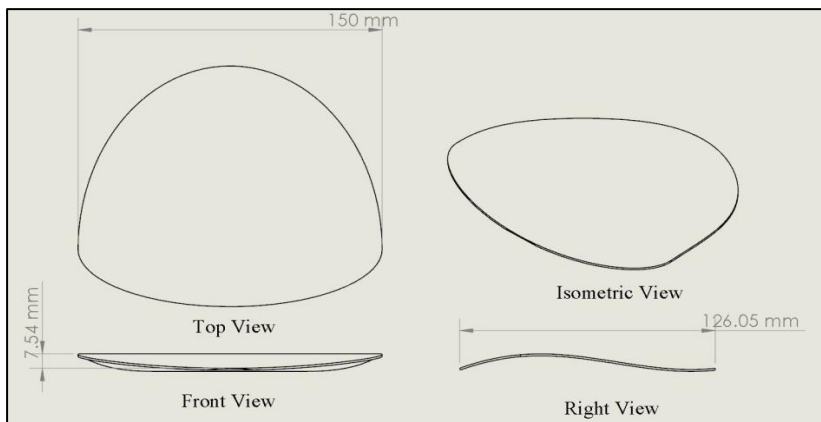


**Fig 2. Zimmerman Wing**

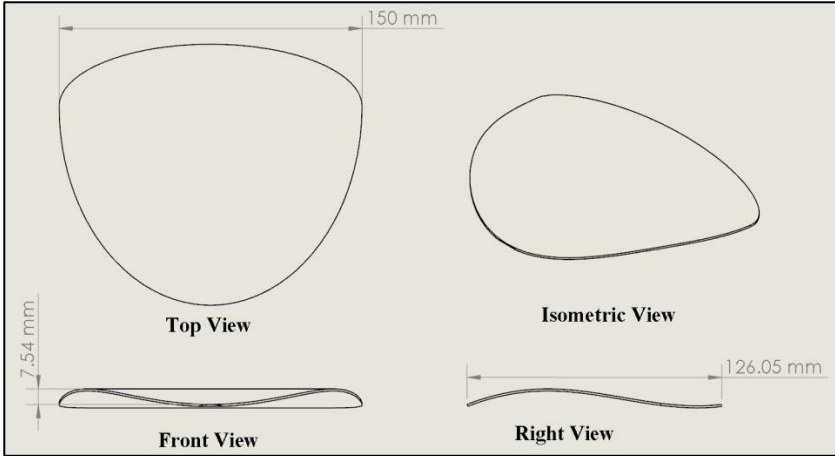


Fig 3. Inverse Zimmerman Wing

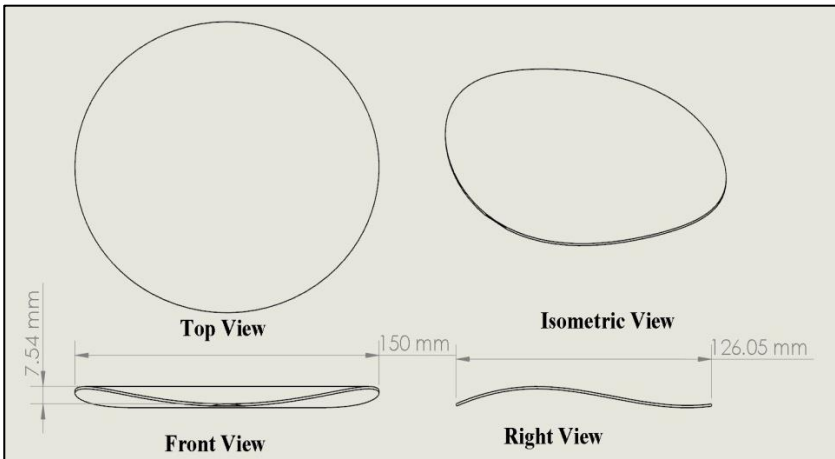


Fig 4. Ellipse Wing.

Thin airfoil was implemented consistently for each wing based the 4th order polynomial equation. The 4th order polynomial equation used for the shape airfoil geometry is given as

$$y = 6E-06x^3 - 0.004x^2 + 0.401x \quad (1)$$

### Mesh generation

The computational flow (CFD) domain, which is built surrounding each MAV wing with a symmetrical condition applied. The unstructured CFD mesh for airflow domain (enclosure) is developed consists of tetrahedral, pyramidal,

hexahedral, and/or prismatic elements with inflation layers. The Inflation layer was well applied especially for mesh detailing near each wing boundaries. Twelve layers of mesh inflation were well developed on the wing wall, with the transition ratio and growth rate at 0.77 and 2.2 respectively. The first cell above the wing surface is set at  $y^+ \leq 1$ . The example of optimized mesh ( $\approx 500,000$  elements) with inflation layers is shown in Fig 5.

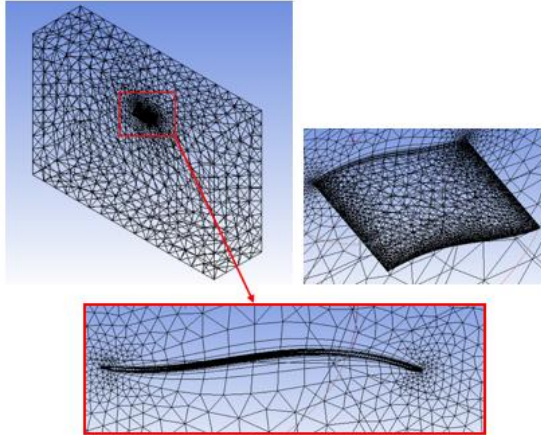


Fig 5. Example of optimized mesh with inflation layers

### **CFD flow boundary conditions**

The symmetrical boundary condition applied on the CFD domain as shown in Fig 6. The location of inlet and outlet indicated by flow vectors (Fig 6). The flow velocity was specified at the inlet with velocity of 9.5 m/s which is equivalent to  $Re = 100,000$  (maximum  $Re$  for MAV operations). Zero pressure boundary condition is implemented at the outlet to ensure airflow continuities. The symmetrical wall and side walls (opposite the symmetrical wall) imposed as symmetrical and slip surface boundary conditions, respectively. Non-slip boundary surface imposed on wing surface and automatic wall function is fully employed to solve the flow viscous effect.

### **MAV wing simulation**

The CFD problems over the Rectangular, Zimmerman, Inverse Zimmerman and Elliptical wing designs were solved based on steady state and incompressible turbulent flow. In this works, the Reynolds Average Navier-Stokes (RANS) equations coupled with SST  $k-\omega$  turbulent model is fully utilized in the solver [13]. The CFD analysis over each wing was set at angle of attack (AOA) range between  $-5^\circ$  to  $30^\circ$  (with  $2^\circ$  interval). The automatic wall function is fully employed to solve the flow viscous effect.

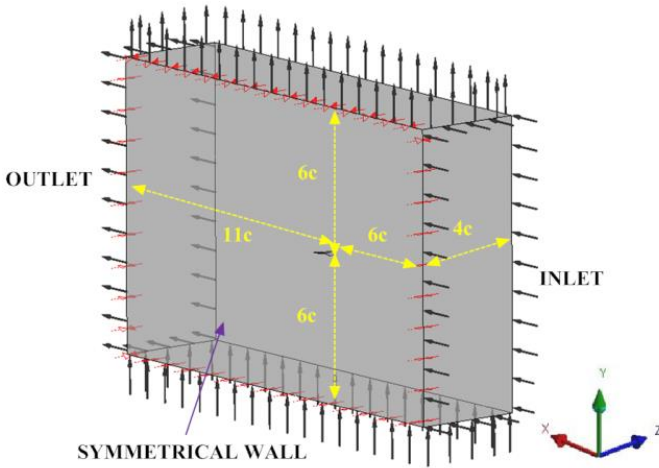


Fig 6. CFD Boundary Conditions

## Results

In this study, the analysis of aerodynamics performances on the Rectangular, Zimmerman, Inverse Zimmerman and Elliptical wings is focusing on the Lift Coefficient ( $C_L$ ), Drag Coefficient ( $C_D$ ) and lift-to-drag ( $C_L/C_D$ ) characteristics.

### Lift Coefficient

Fig. 7 shows the  $C_L$  performances for Rectangular, Zimmerman, Inverse Zimmerman and Elliptical wings. At the pre-stall AoA region, the  $C_L$  curves for all wing increased linearly towards the AoA increment.  $C_L$  magnitude reached its highest point at the wing stall angle ( $AoA_{stall}$ ) before the lift suddenly drop after the  $AoA_{stall}$ .

Based on the zero-lift angle ( $C_{L=0}$ ) analysis, the results showed that Ellipse wing had generate earlier  $C_{L=0}$  compared to the other designs at  $AoA \approx -6^\circ$ . Surprisingly, Zimmerman and Inverse Zimmerman induced almost similar  $C_{L=0}$  at  $AoA \approx -5^\circ$ . While, Rectangular wing delayed  $C_{L=0}$  at  $AoA \approx -3^\circ$ .

Stall angle ( $AoA_{stall}$ ) is a significant point where the MAV wing reach its highest flight envelope. Based on the  $AoA_{stall}$  results, both Ellipse and Inverse Zimmerman wing exhibited the most delayed stall wing at  $AoA_{stall} = 24^\circ$ . Zimmerman Wing induced stall at  $AoA_{stall} = 22^\circ$  which is 8.3% earlier than Ellipse and Inverse Zimmerman. However, Rectangular wing has induced the earliest stall at  $AoA_{stall} = 18^\circ$ .

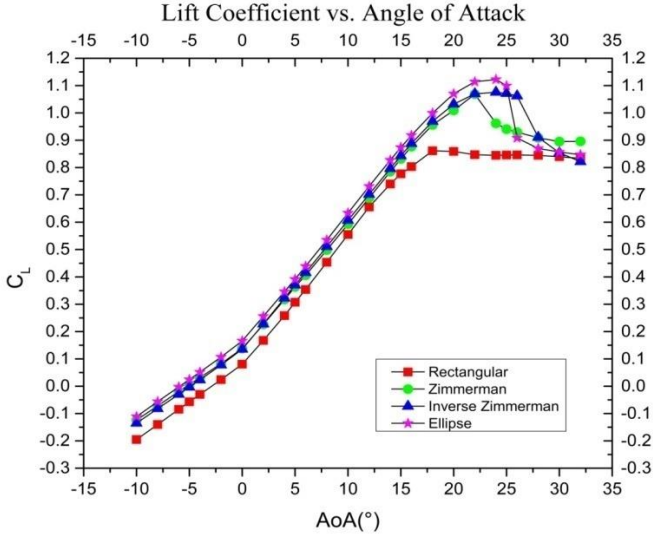


Fig. 7  $C_L$  performances for Rectangular, Zimmerman, Inverse Zimmerman and Elliptical wings

The maximum lift coefficient ( $C_{L_{max}}$ ) is also a significant point for  $C_L$  results in which the point is used to indicate the highest lift distribution induced by the MAV wing. It can be pinpoint through  $AoA_{stall}$  location found at the peak of  $C_L$  curve.

Based on the  $C_L$  curves, it clearly shows that Ellipse wing exhibited the highest  $C_{L_{max}}$  at 1.122. Inverse Zimmerman and Zimmerman wing produced a slightly lower  $C_{L_{max}}$  at 1.076 and 1.069, respectively. However, Rectangular wing induced the lowest  $C_{L_{max}}$  value at 0.861 which is 30.31% lower than the Ellipse wing produced.

Based on  $C_L$  results, one can presume that Ellipse wing has slight advantages in providing better  $C_{L=0}$ ,  $AoA_{stall}$  and  $C_{L_{max}}$  magnitudes among the wings.

### Drag Coefficient

Fig. 8 shows the  $C_D$  performances for Rectangular, Zimmerman, Inverse Zimmerman and Elliptical wings. The results showed that each wing exhibited a slight decrease in  $C_D$  until the curves reached  $C_{D_{min}}$  magnitude before  $AoA=0^\circ$ . However, as the  $AoA$  increase further ( $AoA>0^\circ$ ), each wing exhibited larger  $C_D$  magnitude.

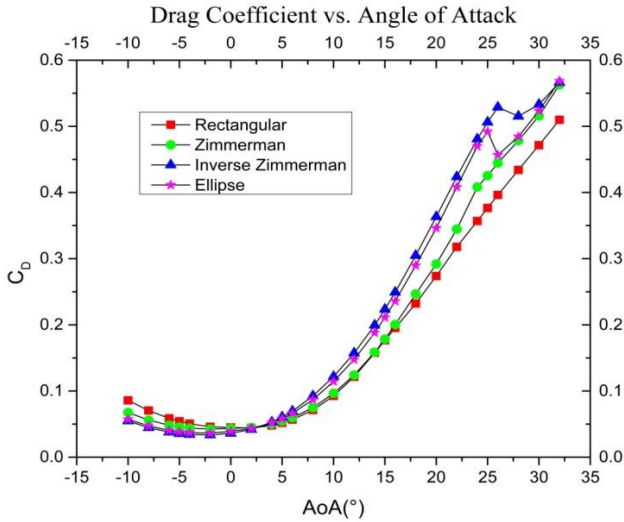


Fig. 8  $C_D$  performances for Rectangular, Zimmerman, Inverse Zimmerman and Elliptical wings

Based on detail  $C_{D_{min}}$  analysis, it shows that Inverse Zimmerman wing generated the lowest  $C_{D_{min}}$  magnitude at 0.033. Ellipse Wing also induced large  $C_{D_{min}}$  magnitude at 0.036 which is 8.45% higher than Inverse Zimmerman produced. However, both Zimmerman and Rectangular wings produced among the largest  $C_{D_{min}}$  magnitude at 0.043 and 0.044, respectively.

Based on detail  $C_D$  analysis at pre-stall region ( $0^\circ$  to  $AoA_{stall}$ ), the results show that  $C_D$  magnitude for Inverse Zimmerman wing increase drastically which at least 32.8% higher than Rectangular wing. Meanwhile, Ellipse and Zimmerman wing also able to produce high  $C_D$  magnitude which is about 26.5% and 6.6% higher than Rectangular wing produced. To detail about the  $C_D$  analysis, the percentage increment  $C_D$  magnitude was investigated at certain pre-stall angle region ( $5^\circ$  to  $25^\circ$ ). Results shows that Rectangular wing have the highest percentage of increment by at least 13.55%. It is followed by Zimmerman and Ellipse Wing at 13.50% and 13.11% respectively. However, Inverse Zimmerman produced the lowest percentage of  $C_D$  increment at 12.62%.

Based on  $C_D$  results, one can presume that Ellipse wing also has advantages by inducing lower  $C_{D_{min}}$  magnitude. However, Inverse Zimmerman emerged to show a slight advantages by providing lower increment in  $C_D$  magnitude towards  $AoA_{stall}$ .

### Moment Coefficient

The aerodynamic investigation on the MAV wing shapes continue the pitching moment coefficient ( $C_M$ ) results as shown in Fig. 9. In this works,  $C_M$  magnitude was measured at leading edge of each wing. In general, the result shows that  $C_M$  for each wing experienced a slight non-linear decrement towards the  $C_{L_{max}}$ . In fact, all  $C_M$  curves experience negative slopes which use to indicate as the initial stability achievement found on each wing.

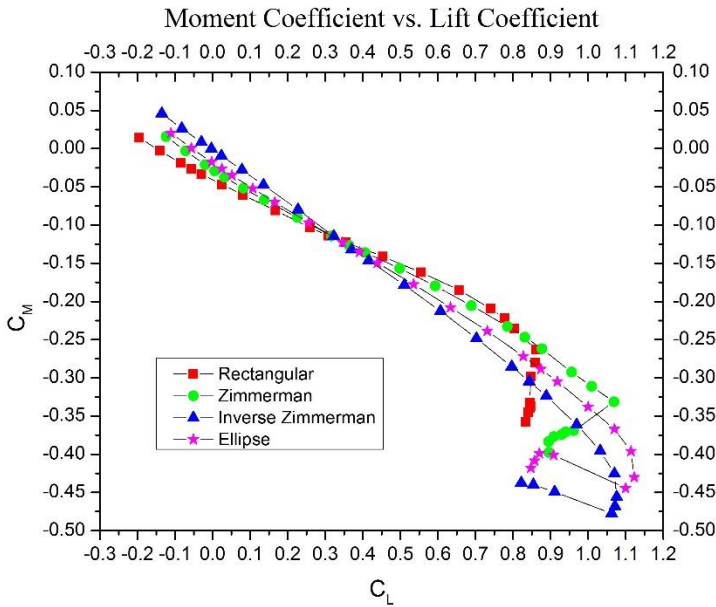


Fig. 9  $C_M$  performances for Rectangular, Zimmerman, Inverse Zimmerman and Elliptical wings

In detail  $C_M$  analysis, an investigation was conducted based on the magnitude of  $C_M$  slopes ( $\Delta C_L / \Delta C_M$ ) taken at AoA region between  $0^\circ$  to  $15^\circ$ . In aerodynamic study, the slope magnitude is used to indicate the level of stability for an aircraft. Stanford shows that steeper  $C_M$  slope means the higher the static stability level achieve on the MAV wing [14].

Based on the magnitude of  $\Delta C_L / \Delta C_M$  results, it shows that Inverse Zimmerman wing generated the steepest  $C_M$  slope at  $\Delta C_L / \Delta C_M = -0.360$ . Then followed by Ellipse and Zimmerman wing which generated about  $\Delta C_L / \Delta C_M = -0.306$  and  $-0.254$  respectively. However, the Rectangular wing generated less steep slope only at  $\Delta C_L / \Delta C_M = -0.241$ . Based on these  $C_M$  results one can conclude that Inverse Zimmerman wing shapes may provide better stability on MAV wing.

### Lift-to-Drag distributions

In aerodynamic study, the magnitude of lift-to-drag ratio ( $C_L/C_D$ ) also recognized parameter to indicate the aerodynamic efficiency of the wing. Fig. 10 shows the  $C_L/C_D$  results for Rectangular, Zimmerman, Inverse Zimmerman and Elliptical wings.

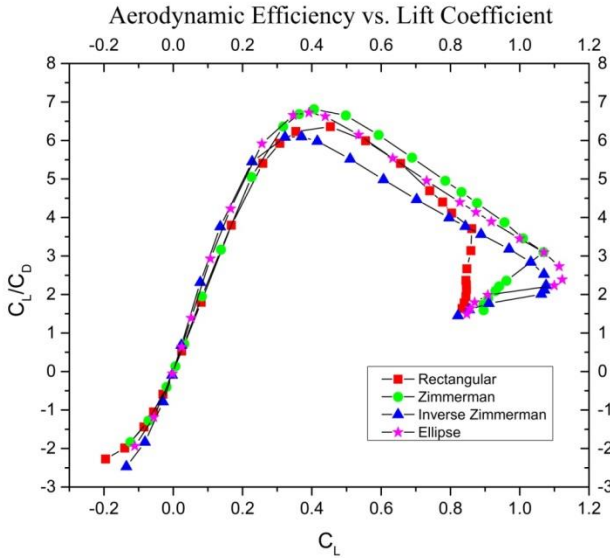


Fig. 10  $C_L/C_D$  performances for Rectangular, Zimmerman, Inverse Zimmerman and Elliptical wings

The  $C_L/C_D$  results show that  $C_L/C_D$  curves for each wing increased linearly as  $C_L$  increased (at  $C_L \leq 0.4$ ). However, as  $C_L/C_D$  curves reached its peak point at  $C_L \approx 0.37 - 0.45$  ranges. The peak point is used to indicate the maximum aerodynamic efficiency ( $C_L/C_{D_{max}}$ ) of each wing. Based on the  $C_L/C_D$  results, it shows that the  $C_L/C_{D_{max}}$  for each wing designs occurred at the early AoA stages (between  $5^\circ$  to  $8^\circ$  or equivalent to  $C_L = 0.37 \sim 0.45$ ). Higher  $C_L/C_{D_{max}}$  magnitude means better aerodynamic efficiency. However, as the AoA increase, the magnitude of  $C_L/C_D$  began to decrease. A detail studies on  $C_L/C_{D_{max}}$  magnitude shows that Zimmerman wing able to produce the highest  $C_L/C_{D_{max}}$  magnitude among the wings at 6.81. This is followed by Ellipse and Rectangular wings at  $C_L/C_{D_{max}} = 6.72$  and 6.36, respectively. Surprisingly, Inverse Zimmerman wing produced the lowest  $C_L/C_{D_{max}}$  magnitude among the wings at  $C_L/C_{D_{max}} = 6.09$ . Based on these  $C_L/C_{D_{max}}$  results, one can presume that Zimmerman has the best

aerodynamic efficiency among the wing design. Based on these results, one can presume that Zimmerman wing has the highest potential to be adopted as MAV wing due to its optimal aerodynamic efficiency.

## **Conclusion**

The aerodynamics analysis on the Rectangular, Zimmerman, Inverse Zimmerman and Elliptical wings has been conducted by focusing on the Lift Coefficient ( $C_L$ ), Drag Coefficient ( $C_D$ ) and lift-to-drag ( $C_L/C_D$ ) distributions. The results show that Ellipse wing has slight advantages in providing better  $C_{L=0}$ ,  $AoA_{stall}$  and  $C_{L_{max}}$  magnitudes among the wings. Analysis shows that Ellipse wing induced  $C_{L_{max}}$  at 1.12 which is at least 4.33% higher than the other wing designs. Based on  $C_D$  analysis, Ellipse wing exhibited 8.45% lower  $C_{D_{min}}$  magnitude (at 0.033) compared to Rectangular, Zimmerman and Inverse Zimmerman wing produced. However, Inverse Zimmerman also shows a potential ability by providing lower increment in  $C_D$  and better stability due to steeper  $C_M$  slopes. Inverse Zimmerman Wing exhibited the steepest curve slope value at -0.36 which is 17.39% better than the other wings. Despite advantages found in Ellipse and Inverse Zimmerman wing, Zimmerman has induce the best aerodynamic efficiency among the wing design. Zimmerman Wing recorded the highest  $C_L/C_D$  value at 6.80 and at least 1.35% higher than to the other wing. This result further indicates its potential application to be adopted as future MAV wing. In future works, a wind tunnel works will be carried out to validate the simulation findings.

## **Acknowledgement**

The authors acknowledge technical and financial support from Universiti Teknologi MARA and the Government of Malaysia via the sponsorship by the Malaysia Ministry of Higher Education's Fundamental Research Grant Scheme (FRGS) (600-RMI/FRGS 5/3 (152/2014)).

## **References**

- [1] Ray, C. W. Modeling, Control, and Estimation of Flexible, Aerodynamic Structures. (ProQuest Dissertations and Theses ,2012).
- [2] Moore, R. J. D., Dantu, K., Barrows, G. L. & Nagpal, R. "Autonomous MAV guidance with a lightweight omnidirectional vision sensor" Proceedings of IEEE International Conference on Robotics and Automation 3856–3861 (2014).
- [3] Bronz, M., Moschetta, J. M., Brisset, P. & Gorez, M. "Towards a long endurance MAV". International Journal of Micro Air Vehicles 1, 244–245 (2009).

- [4] Ismail, N. I., Zulkifli, A. H., Abdullah, M. Z., Basri, M. H. M. & Pahmi, M. A. A. H. "Evolution Of Monoplane Fixed Wing Micro Air Vehicle's Shape And Design Review". Proceedings of 2nd. International Conference on Arts, Social Sciences & Technology (ICAST2012) 1–13 (2012).
- [5] Ismail, N. I. Aerodynamic Performances of Twist Morphing MAV Wing. (PhD Thesis Dissertation, Universiti Teknologi MARA, 2015).
- [6] Ismail, N. I., Zulkifli, A., Talib, R., Yusoff, H. & Tasin, M. A. "Vortex structure on twist-morphing micro air vehicle wings". International Journal of Micro Air Vehicles 8, 194–205 (2016).
- [7] Ahmed, M. R. & Abdelrahman, M. M. "Optimal wing twist distribution for roll control of MAVs." The Aeronautical Journal 115, 641–649 (2011).
- [8]. Ismail, N. I., Zulkifli, a. H., Abdullah, M. Z., Basri, M. H. & Abdullah, N. S. "Optimization of aerodynamic efficiency for twist morphing MAV wing". Chinese Journal of Aeronautics 27, 475–487 (2014).
- [9]. Shetty, P., Subrahmanya, M. B., Kulkarni, D. S. & Rajani, B. N. "CFD Simulation of Flow Past Micro Air Vehicle Wings" Proceedings of Applied Aerodynamics and Design of Aerospace Vehicle (SAROD), 13, 1-10, (2013).
- [10] Zuo, L. X. & Wang, J. J. "Planform and Flexibility on Lift "Characteristics for Flow over Low-Aspect Ratio Wings". Journal of Aerospace Engineering 2(3), 55–61 (2010).
- [11]. Radmanesh, M., Nematollahi, O. & Hassanalian, M. A "Novel Strategy for Designing and Manufacturing a Fixed Wing MAV for the Purpose of Increasing Maneuverability and Stability in Longitudinal Axis" Journal of Applied Fluid Mechanics 7, 435–446 (2014).
- [12]. Zuo, L. X. & Wang, J. J. "Planform and Flexibility on Lift Characteristics for Flow over Low-Aspect Ratio Wings" Journal of Aerospace Engineering, 55–61 (2010).
- [13] Ismail, N. I. Aerodynamic Performances and Flow Structure Investigations On Active Twist Morphing MAV Wing. (Universiti Teknologi MARA, 2014).
- [14] Ismail, N. I. et al. "Computational Aerodynamic Analysis on Perimeter Reinforced (PR)-Compliant Wing" Chinese Journal of Aeronautics 26, 1093–1105 (2013).